Myelin sheath structure and regeneration in peripheral nerve injury repair

Bin Liu[a,b,1], Wang Xin[a], Jian-Rong Tan[a], Rui-Ping Zhu[a], Ting Li[a], Dan Wang[a], Sha-Sha Kan[a], Ding-Kui Xiong[c], Huan-Huan Li[a], Meng-Meng Zhang[a], Huan-Huan Sun[a], William Wagstaff[b], Chan Zhou[c,1], Zhi-Jian Wang[a,1], Yao-Guang Zhang[a], and Tong-Chuan He[b]

[a]Key Laboratory of Freshwater Fish Reproduction and Development, Ministry of Education, School of Life Sciences, Southwest University, 400715 Chongqing, China; [b]Molecular Oncology Laboratory, Department of Orthopaedic Surgery and Rehabilitation Medicine, University of Chicago Medical Center, Chicago, IL 60637; and [c]Institute for Silk and Related Biomaterials Research, Chongqing Academy of Animal Science, 402460 Chongqing, China

Edited by Lawrence Steinman, Stanford University School of Medicine, Stanford, CA, and approved September 24, 2019 (received for review June 25, 2019)

Observing the structure and regeneration of the myelin sheath in peripheral nerves following injury and during repair would help in understanding the pathogenesis and treatment of neurological diseases caused by an abnormal myelin sheath. In the present study, transmission electron microscopy, immunofluorescence staining, and transcriptome analyses were used to investigate the structure and regeneration of the myelin sheath after end-to-end anastomosis, autologous nerve transplantation, and nerve tube transplantation in a rat model of sciatic nerve injury, with normal optic nerve, oculomotor nerve, sciatic nerve, and Schwann cells used as controls. The results suggested that the double-bilayer was the structural unit that constituted the myelin sheath. The major feature during regeneration was the compaction of the myelin sheath, wherein the distance between the 2 layers of cell membrane in the double-bilayer became shorter and the adjacent double-bilayers tightly closed together and formed the major dense line. The expression level of myelin basic protein was positively correlated with the formation of the major dense line, and the compacted myelin sheath could not be formed without the anchoring of the lipophilin particles to the myelin sheath.

myelin sheath | myelin basic protein (MBP) | lipophilin | anchoring particle | major dense line (MDL)

Structural abnormalities in the myelin sheath (1) can lead to a variety of neurological conditions (2–5), such as Alzheimer's disease (6), Pelizaeus-Merzbacher disease (7), multiple sclerosis (8), experimental allergic encephalomyelitis (9), and pathological neuropathic pain (10). The morphology of the myelin sheath differs slightly among the brain, spinal cord, and peripheral nerves, but all have an axon that is concentrically wrapped by glial cells, with the myelin sheath formed on the outer surface of the axon. A comprehensive understanding of the structure and regeneration of the myelin sheath in peripheral nerves at baseline and during injury repair would help to understand the pathogenesis and treatment of various neurological diseases. There is a large body of existing literature about the structure and formation of the myelin sheath (11–22), but there is confusion regarding some issues, such as the development and roles of major dense lines (MDL), myelin basic protein (MBP), myelin compaction, and anchoring.

Among the peripheral nerves (23, 24), there are afferent nerves composed of sensory nerve fibers (such as optic nerves), efferent nerves composed of motor nerve fibers (such as oculomotor nerves), and nerves composed of both sensory nerve fibers and motor nerve fibers (such as the sciatic nerve). Observing and comparing the morphology of the optic nerve, oculomotor nerve, and sciatic nerve myelin may provide a more comprehensive understanding of the structure of the myelin sheath.

There are 3 main strategies currently employed to repair peripheral nerve injury: Namely, end-to-end anastomosis for nerve rupture, autologous nerve transplantation, and artificial nerve transplantation for nerve defects. Demyelination, phagocytosis, and remyelination were previously observed on the 5th, 14th, and 28th days after surgery, respectively, following the repair of a 1-mm sciatic nerve defect in mice (25). Therefore, the first 4 wk after surgical repair of a sciatic nerve injury might be a suitable period for observing remyelination.

During the experimental repair of peripheral nerve injury (26–28), the sciatic nerve is usually used as the target (29–32). The sciatic nerve contains both afferent and efferent nerve fibers. Therefore, whether the afferent and efferent nerve fibers can be distinguished based on morphological differences would be a question of interest in nerve injury repair.

In the brain and spinal cord, the glial cells are mainly oligodendrocytes (4), while in the peripheral nerves, the glial cells are Schwann cells. There are 4 main types of mature Schwann cells. The satellite Schwann cells are mainly located in the ganglia, perisynaptic Schwann cells (also known as terminal Schwann cells) are located at the nerve terminals, and myelinating Schwann cells (MSC) and nonmyelinating Schwann cells (NMSC) are located in the peripheral nerves. An MSC envelops an axon to form a multilayer myelin sheath, while an NMSC wraps a plurality of axons (C-fiber) to form a Remark bundle (33). Therefore, in any study of the structure and regeneration (34–36) of the myelin sheath in peripheral nerves, it is necessary to pay attention to both MSCs and NMSCs. Typically, these are distinguished by using

Significance

Afferent and efferent nerve fibers cannot be distinguished based on the axonal diameter or the presence of the Remark bundle. The compaction of the myelin sheath involves 2 steps: 1) The distance between the 2 layers of cell membranes in the double-bilayer decreases; 2) the adjacent double-bilayers close to form MDL. The expression of MBP is positively correlated with the formation of the MDL. Anchoring of the myelin sheath by lipophilin particles might be required for the formation of a compacted myelin sheath. The abnormalities in nerve fiber structure observed in autologous nerve grafts do not appear to be related to either MBP or lipophilin, so further research is needed to determine their causes.

Author contributions: B.L., C.Z., Z.-J.W., Y.-G.Z., and T.-C.H. designed research; B.L., W.X., J.-R.T., R.-P.Z., T.L., D.W., S.-S.K., D.-K.X., H.-H.L., M.-M.Z., H.-H.S., and C.Z. performed research; T.-C.H. contributed new reagents/analytic tools; B.L., W.W., C.Z., Z.-J.W., Y.-G.Z., and T.-C.H. analyzed data; and B.L. wrote the paper.

The authors declare no competing interest.

This article is a PNAS Direct Submission.

[1]To whom correspondence may be addressed. Email: xytom@swu.edu.cn, chanzhoum@163.com, or wangzj@swu.edu.cn.

This article contains supporting information online at www.pnas.org/lookup/suppl/doi:10.1073/pnas.1910292116/-/DCSupplemental.

First published October 14, 2019.

MBP and glial fibrillary acidic protein (GFAP) as markers, respectively (32, 37, 38).

Studies on Shiverer (*Shi*/*Shi*) mice have shown that MBP is 1 of the proteins that is important for maintaining the normal structure of the myelin sheath. Shiverer mice are homozygous for autosomal recessive mutations, and exhibit distinct tremors (shivering), convulsions, and early death (39). In these mice, the myelin sheath of the central nervous system is characterized by a lack of MDL (40). In a previous study, there was no MDL in most of the myelin sheaths from 40-d-old Shiverer mouse corpus callosums, but there was MDL in the myelin sheath in the ventral and dorsal roots of their spinal cords (40, 41). Of note, the myelin structure was grossly normal in the spinal nerve roots and sciatic nerves of the Shiverer mice at ∼35 d of age (42). These observations indicate that the myelin structure of the Shiverer's peripheral nerves is normal, so it was believed that this mutation does not completely eliminate the ability of the mice to produce certain types of myelin sheath (41).

MBP is closely related to the formation of the MDL. The decrease in the expression of MBP at different stages and in different locations due to partial deletion of the MBP gene is an important feature of the Shiverer nervous system (1, 15, 39, 40, 43–47). MBP is also known as encephalitogenic protein or A1 protein. In the central nervous system, MBP accounts for ∼30% of the total protein involved in the formation of myelin in the sheath (15, 39), while in Shiverer mouse brain extracts, the MBP content was less than 3% of the normal content; therefore, Shiverer mice lack sufficient MBP (39). There are 4 main isoforms of MBCs (45, 48), with molecular mass of 21.5, 18.5, 17, and 14 kDa, respectively, and its amino acid sequence is highly conserved throughout different species (43). In the central and peripheral nerves of different species, these isoforms are all present at the same time, but the proportions are different (15, 44, 49–51). MBP undergoes acetylation, methylation, and phosphorylation during the formation of a 3D structure, and its structure changes under certain conditions (15, 49–51). The stick-like structure model (15, 50) of MBP is useful to explain the compaction between 2 layers of cell membranes in the myelin structural unit (Fig. 1). These isoforms are the product of alternative splicing of a single gene located on chromosome 18 (39, 43–45, 47).

The membrane constituting the myelin sheath is composed of protein (20 to 30%) and lipids (70 to 80%) (15). The proteins include MBP (30 to 40%) (39) and proteolipid proteins (PLP) (15). Lipophilin accounts for about 50% of the PLP (15). MBP is associated with the compaction of the myelin sheath, and lipophilin might be associated with the anchoring of the myelin sheath (Fig. 1).

The electrostatic and hydrophobic interactions between MBP and membrane lipids are the main reasons for the formation of the double-bilayer structure and the stability of the myelin sheath (16). The glial cell membrane (52, 53) is composed of a lipid bilayer and the proteins located thereon. MBP is located on the inner surface of the membrane (cytoplasmic surface) (43), making it positively charged and hydrophobic. MBP and the negatively charged lipid molecules attract each other, thus "adsorbing" onto the inner surface of the cell membrane (Fig. 1). During the formation of the myelin sheath, glial cells are squashed into lamellae, the 2 layers of cell membranes are brought into proximity to each other, and the positive charge of MBP and the negative charge of the opposite cell membrane lipids attract each other (13) so that the 2 layers of cell membranes are more stably combined. Together, these form a double-bilayer structure consisting of 2 layers of cell membranes, each of which has 2 layers of lipid molecules (16, 40, 54). In the double-bilayer structure, the 2 layers of cell membranes are separated by 3 to 8 nm and are filled by the cytoplasm of glial cells. This is the structural unit that constitutes the myelin sheath and is called a MDL (16, 40) (Fig. 1). However, the relationship between the double-layer structure and the compaction of the myelin and the MDL remains to be fully elucidated.

A large number of uniformly distributed particles were observed in the myelin sheaths of human white matter (15), rat sciatic nerve (55), and 38-d-old Shiverer spinal cord (40) in freeze-fracture replicas. Those particles are radially distributed and pass through multiple double-bilayers (55). These observations indicated that the particles were important for maintaining the integrity of the myelin sheath, but were not formed by the MBP. Similar particles were also found in vesicles of egg phosphatidylcholine containing 20% lipophilin, indicating that these particles were formed by lipophilin (15). Lipophilin is a distinct component of the PLP fraction, and is not equivalent to PLP (15, 56).

To observe the structure and regeneration of the myelin sheath during rat (*SI Appendix*, Section S1) peripheral nerve injury repair, transmission electron microscopy (TEM) observation (*SI Appendix*, Section S2), immunofluorescence staining (*SI Appendix*, Section S3), and transcriptome analyses (*SI Appendix*, Sections S4 and S5) of the myelin sheath were performed following end-to-end anastomosis, autologous nerve transplantation, and nerve tube (*SI Appendix*, Section S6) transplantation in a rat model of sciatic nerve injury (*SI Appendix*, Section S7), with the optic nerve, oculomotor nerve, sciatic nerve (*SI Appendix*, Section S8), and Schwann cells (*SI Appendix*, Section S9) used as controls.

Results

The Structure of the Myelin Sheath in Different Types of Nerves. Immunofluorescence staining for NF200, an axonal marker, showed that the axons have different diameters within each nerve (*SI Appendix*, Fig. S1*A*). The number and distribution of axon diameters in different nerves also differed. Small-diameter axons predominated in the optic nerve, while large-diameter axons were predominant in the oculomotor nerve, and the proportion of small-diameter axons in the sciatic nerve was slightly higher than that in the oculomotor nerve. NGFR P75 is a marker of both MSCs and NMSCs. As shown in *SI Appendix*, Fig. S1*A*, there was a

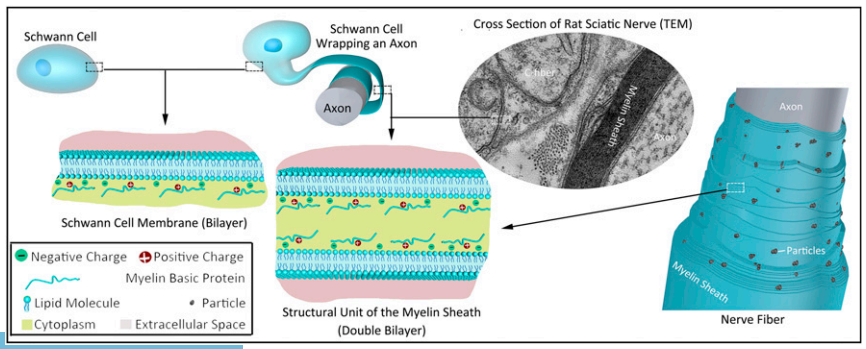

Fig. 1. Structural unit of the myelin sheath (double- bilayer) and particles.

difference in the distribution of Schwann cells in different nerves. Since Schwann cells are wrapped around axons, differences in the axon distribution would naturally lead to differences in the Schwann cell distribution.

GFAP is a marker of NMSCs. Immunofluorescence staining showed that the number of NMSCs in the sciatic nerve was significantly higher than in the optic nerve and oculomotor nerve (*SI Appendix*, Fig. S1*B*). GFAP staining also showed positivity in the primary cultured Schwann cells (*SI Appendix*, Fig. S1*C*). MBP101 is a marker of MSCs. Immunofluorescence staining showed that the distribution of MSCs in the sciatic nerve was significantly lower than in the optic nerve and oculomotor nerve. There was also some positive MBP101 staining in the primary cultured Schwann cells (*SI Appendix*, Fig. S1*C*).

There were significantly fewer NMSCs than MSCs in the optic nerve and oculomotor nerves, although the proportions of the areas of these 2 cells in the cross section of the sciatic nerve was roughly equal. The primary cultured Schwann cells exhibited characteristics of both MSCs and NMSCs.

TEM observation showed significant differences in the thickness of the myelin sheath in the cross-sections of the optic nerve, oculomotor nerve, and sciatic nerve. In the oculomotor nerve and the sciatic nerve, there were myelin sheaths of different thicknesses. In the optic nerve, most of the myelin sheaths were thinner than those of the oculomotor nerve and the sciatic nerve (Fig. 2*A*). The Remark bundle (Fig. 2 *A*, *III*) was more easily observed in the cross-sections of the oculomotor and sciatic nerves than the optic nerve. Particles (indicated by the white arrowhead in Fig. 2*B*) were observed on the myelin sheaths of all 3 types of nerves. The MDL was prominent in the multilayered myelin sheath composed of multilayered structural units (the double-bilayer in Fig. 1) formed by MSCs (Fig. 2*B*). In contrast, in the cross-sections of the sciatic nerve (Fig. 2*C*), the nonlayered myelin sheath (between 2 black arrowheads in Fig. 2*C*) formed by the NMSCs surrounding the C-fiber was composed of a single layer of the structural unit, and the MDL was not significant.

Myelin Sheath Structure during Peripheral Nerve Injury Repair. End-to-end anastomosis of the broken sciatic nerve was performed in a rat model of nerve injury (10 mm), and frozen sections were made for immunofluorescence staining on the 30th day after the surgery. The results showed that both MBP101 and GFAP were positive in both the distal and proximal sciatic nerves (*SI Appendix*, Fig. S2*A*). In other rats, autologous nerve transplantation was performed on the 10-mm defect of the sciatic nerve. Immunofluorescence staining was again performed on the 30th day after surgery. Both MBP101 and GFAP were positive in the distal end, proximal end, and graft of the sciatic nerve (*SI Appendix*, Fig. S2*B*). Nerve tube grafting was performed on the 10-mm defect of the sciatic nerve in a third group of rats. The growth cones were taken on the 30th day after surgery, and the immunofluorescence staining of frozen sections was performed. The results showed that NF200, NGFR P75, MBP101, and GFAP were all positive (Fig. 3).

TEM observation was performed on the 30th day after end-to-end anastomosis. The results showed that there were no significant abnormalities in the structure of myelin sheath at either the distal end or proximal end of the sciatic nerve (*SI Appendix*, Fig. S3). On the 30th day after autologous nerve transplantation and nerve tube transplantation, the structure of the myelin sheath was not significantly abnormal in either the distal or proximal ends of the sciatic nerves. Some structurally abnormal myelin sheath was observed when the graft was subjected to TEM observation on the 30th day after autologous nerve transplantation (Fig. 4*A*). All of the myelin sheaths (labeled M1, M2, M3, and M4 in Fig. 4*A*) had MDL and particles. M1 and M2 are bridged by a cell membrane (white arrow in Fig. 4*A*), indicating that they were formed by the same Schwann cell, while M2 is located inside M1 and they have axons inside. M3 and M4 are also connected by a cell membrane (white arrow in Fig. 4*A*), indicating that they were also formed by the same Schwann cell, but they have no axons inside. On the 30th day after nerve tube transplantation, myelin sheaths of different diameters (Fig. 4*B*) were observed in the growth cone (Fig. 3), and these myelin sheaths were relatively loose. They had MDL but no anchoring particles (Fig. 4*C*).

Lipophilin, MBP, GFAP, NF200, and NGFR P75 Expression during Sciatic Nerve Injury Repair. As shown in Fig. 5, the relative expression levels of lipophilin and MBP in each group were lower than those in the normal sciatic nerve at each time point examined. At all timepoints, the order of expression was Schwann cell < nerve tube transplantation < autologous nerve transplantation < end-to-end anastomosis.

There was no myelin sheath in the Schwann cells cultured in vitro, and the nerve injured in the 3 experimental groups was in the repair stage, so the number of myelin sheaths in these samples was lower than in the normal sciatic nerve samples.

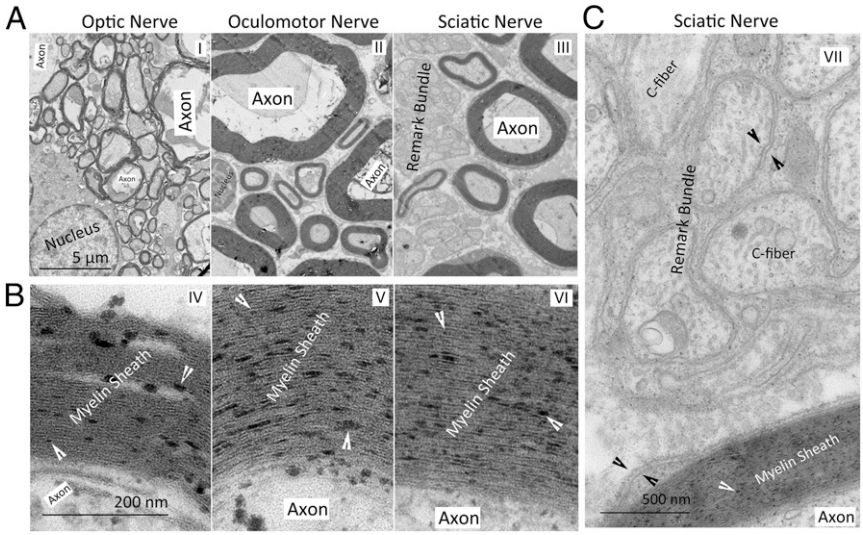

Fig. 2. TEM images of cross-sections of the optic nerve, oculomotor nerve, and sciatic nerve. (*A*) Myelinated axons and Remark bundles. (*B*) Anchoring particles (indicated by white arrowheads) in the myelin sheath. (*C*) Anchoring particles, C-fibers in a Remark bundle and the double bilayer (between the 2 black arrowheads).

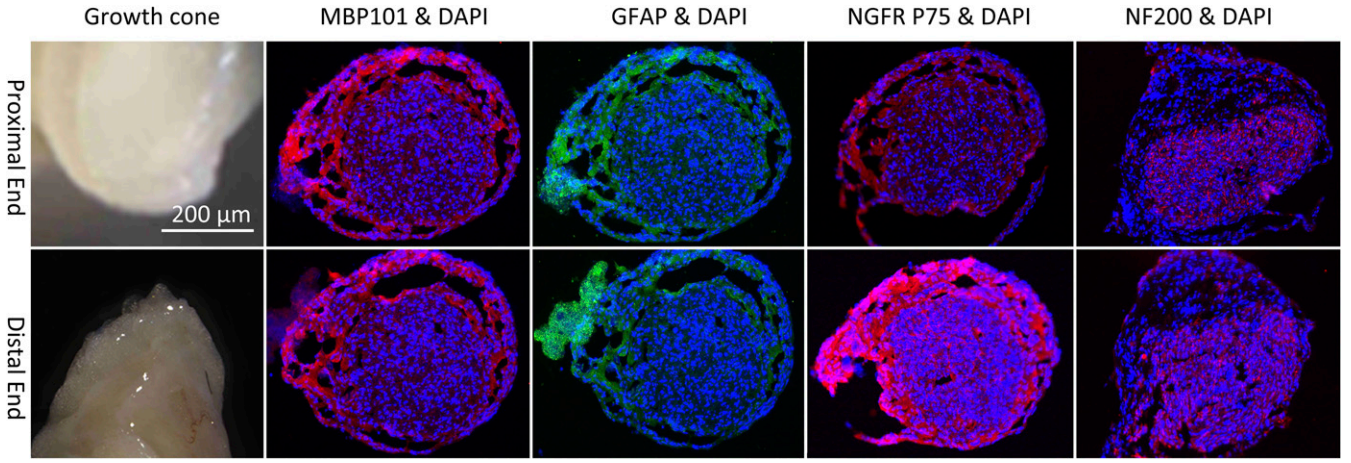

Fig. 3. DAPI, MBP101, GFAP NGFR P75, and NF200 immunofluorescent staining of the cross-sections of growth cones in the nerve tube obtained on the 30th day after transplantation.

In general, end-to-end anastomosis leads to easier repair than autologous nerve transplantation, and autologous nerve transplantation is superior to nerve tube transplantation. The order of difficulty in repairing these nerve injuries was consistent with the differences in the expression of lipophilin and MBP in each group as mentioned above. Therefore, the differences in the expression levels of lipophilin and MBP in each group were positively correlated with the number of myelin sheaths in each group.

We also noted that the relative expression levels of NGFR P75 and GFAP were higher than those of normal sciatic nerve at each time point in each group, and the expression level was the lowest in the Schwann cell group (Fig. 5). Up-regulation of NGFR P75 and GFAP expression means that the Schwann cells were actively proliferating, which was expected, because both cultured Schwann cells and the active repair of peripheral nerve injury are accompanied by cell division.

The relative expression levels of GFAP on day 7 and day 14 were ranked as follows: Nerve tube transplantation < autologous nerve transplantation < end-to-end anastomosis. On day 30 this order had changed to: End-to-end anastomosis < autologous nerve transplantation < nerve tube transplantation. The relative expression levels of NGFR P75 did not show obvious trends either based on the group or the time point. The NF200 expression was almost always lower in each of the groups at each time point compared to the expression in the normal sciatic nerve. There were no obvious trends in the expression level of NF200 based on either time or group.

In the Schwann cells cultured in vitro, the expression level of NF200 was lower than that of the normal sciatic nerve, which indicated that the expression level of NF200 was positively correlated with the content of axons (Fig. 5). On day 14 after autologous nerve transplantation and on day 30 after nerve tube transplantation, the expression of NF200 was higher than that of normal sciatic nerve, indicating that there was active axon growth in these groups. It also showed that the repair activities have different characteristics, and occur over a different time course (Fig. 5).

Discussion

The Diameter of the Axons and the Structure of the Myelin Sheath Could Not Be Used to Accurately Distinguish between the Afferent and Efferent Nerve Fibers, but Small-Diameter Axons May Be a Structural Feature of Afferent Nerve Fibers. The nerve fibers in the optic nerve are afferent nerve fibers with both small- and large-diameter axons, but mainly small-diameter axons. The nerve fibers in the oculomotor nerve are efferent nerve fibers, with both small- and large- diameter axons, but mainly large-diameter axons. The nerve fibers in the sciatic nerve contain both afferent and efferent nerve fibers, and have small- and large-diameter axons, but predominantly large-diameter axons (*SI Appendix*, Fig. S1*A*). These observations indicated that it might be not possible to distinguish between afferent and efferent nerve fibers based solely on the axon

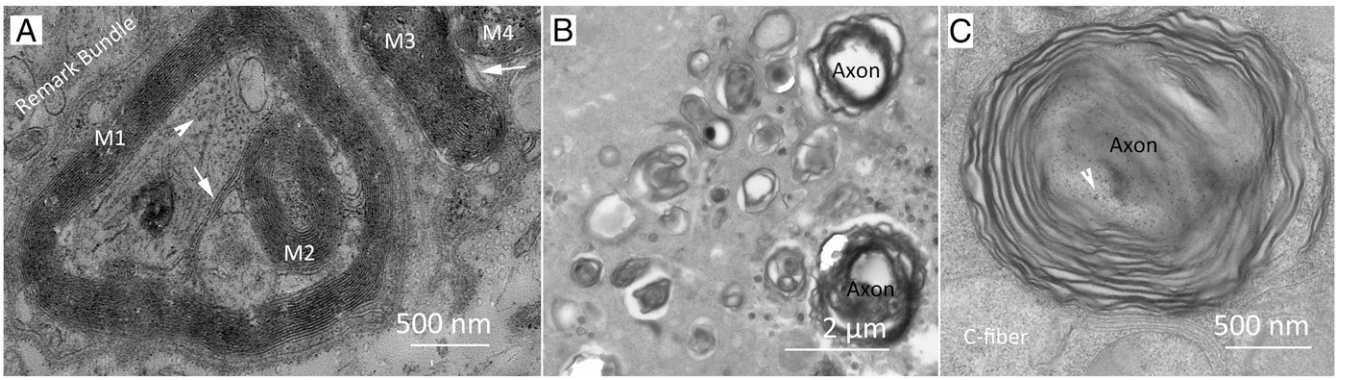

Fig. 4. TEM images of the cross-sections of samples obtained on the 30th day after surgery. (*A*) Abnormal myelin sheath structures in the graft of autologous nerve transplantation. White arrowheads in both (*A*) and (*C*) indicate neurofilament in the axon. White arrows indicated a bridge between 2 myelin sheaths (M1 and M2 or M3 and M4). (*B* and *C*) Loose myelin sheaths with no anchoring particles were present in the nerve fibers growing in the nerve tube.

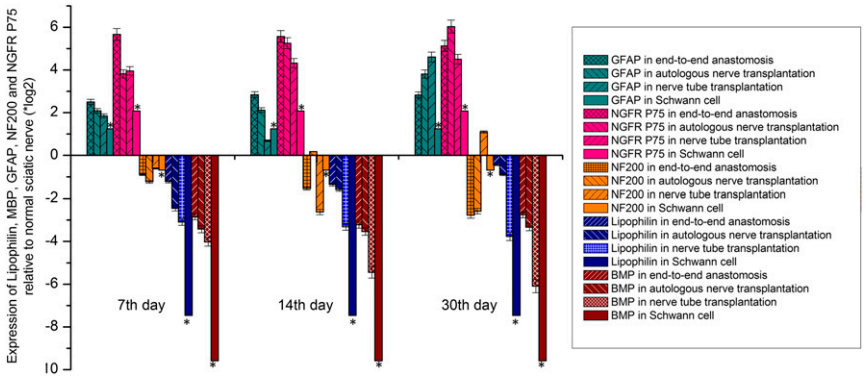

Fig. 5. The expression levels of lipophilin, MBP, GFAP, NF200, and NGFR P75 relative to normal sciatic nerve in the end-to-end anastomosis, autologous nerve transplantation, and nerve tube transplantation groups and in primary cultured Schwann cells (SD = 5% mean ± SEM, $n = 3$, t test). The statistical analysis indicated that there were significant differences among the groups at the same time point, there were also differences in the same group at different time points, with the exception of the cultured Schwann cells $*P < 0.05$.

diameter. However, during the repair of peripheral nerve injury, if there is no regeneration of small-diameter axons, it might indicate that the afferent nerve fibers are not repaired.

MSC and NMSC Are Present in Both Afferent and Efferent Nerve Fibers; the Multiple Layers of the Double-Bilayer and the Remark Bundle Are Distinguishing Features of the MSC and NMSC, Respectively. The C-fiber in the Remark bundle was wrapped by a single layer of double-bilayer. In the afferent nerve fibers (optical nerve), efferent nerve fibers (oculomotor nerve), and sciatic nerve, we observed myelin sheaths containing a single axon, and Remark bundles (Fig. 2 *A* and *C*). These findings indicate that all of 3 types contain both MSCs and NMSCs. Although the myelin sheath formed by MSCs differed in thickness and diameter, it was composed of multilamellar double- bilayer. In the Remark bundle formed by NMSCs, only 1 layer of double-bilayer was wrapped on the outside of each C-fiber (Fig. 2 *A* and *C*). These structural differences could be used to distinguish between MSCs and NMSCs.

The Compaction of the Multilayered Myelin Sheath Might Mean That the Distance Between the 2 Layers of Cell Membranes in the Double-Bilayer Became Shorter and Adjacent Double-Bilayers Closed Together, Thus Forming the MDL. Since the presence of cytoplasm between the 2 layers of cell membranes in the structural unit (Fig. 1) determines that there would be a gap between the 2 membranes, the gap present in the multilayered myelin sheath (Fig. 2*B*) should be cytoplasm in double-bilayers. There was no MDL in the monolayered myelin sheath in the Remark bundle. When the multilamellar myelin sheath (Fig. 2*B*) was compared with the monolayer myelin sheath (Fig. 2*C*), the distance between the 2 layers of cell membranes in the structural unit of the multilamellar myelin sheath was significantly shorter than that in the monolayer myelin sheath, and adjacent structural units were in close proximity to each other to form the MDL. Therefore, the compaction of the myelin sheath (12–14, 20) appears to include 2 steps, namely the shortening of the distance between the 2 layers of the membrane in the double-bilayer and the formation of the MDL.

The Expression Level of MBP Is Positively Correlated with the Formation of the MDL. Compared to the loose myelin sheath (Fig. 4*C*), the myelin sheath of normal peripheral nerves (Fig. 2) is denser—that is, compacted—myelin sheath. In autologous nerve grafts and nerve tube grafts, the expression of MBP in the recipient sciatic nerve was lower than that in the normal sciatic nerve. Furthermore, the expression of MBP in the nerve tube group was lower than that in the autologous nerve graft (Fig. 5), although there were MDL present in both. However, the MDL in the nerve tube group were abnormal (Fig. 4*C*). It was previously reported that there was also MDL in the myelin sheath of the Shiverer mice lacking MBP (40–42). These observations suggest that the expression level of MBP was positively correlated with the number of MDL formed (1, 15, 22, 23, 40, 44–47).

The Anchoring of Myelin Sheath by Lipophilin Particles Was the Main Reason for the Formation of Compacted Myelin. Although there were major dense lines in the growth cone of the nerve tube group (Fig. 4*C*), the myelin sheath was looser compared with the other groups (Fig. 2) and there were no particles on it. In addition, the nerve tube group had the lowest lipophilin expression (Fig. 5). These suggested that compacted myelin could not be formed without particles. Moreover, MBP was located on the inner surface of the cell membrane (cytoplasmic surface) instead of the outer surface of the structural unit (43), which cannot pass through multilayer structural units in the radial direction (Fig. 1). In contrast, lipophilin can form particles in vitro (15), so the particles are likely made of lipophilin rather than MBP.

Existing Models of Myelin Structure Do Not Adequately Explain the Abnormalities in the Structure of Nerve Fibers Observed in Autologous Nerve Grafts. The nerve fibers regenerated in the autologous nerve graft group (Fig. 4*A*) had structural abnormalities, although the structure of their myelin sheath was normal: That is, the myelin sheath was compacted and had the major dense lines and anchoring particles. These structural anomalies were: 1) A Schwann cell that formed 2 myelin sheaths; 2) a myelin sheath was contained within another myelin sheath; and 3) a myelin sheath without an axon in it. Since these myelin sheaths were compacted and had major dense lines and anchoring particles, this suggested that these abnormal structures might not be determined by MBP and lipophilin, but by other factors, so further research is needed to identify these factors and their roles (13, 14, 33).

Conclusion

The difference in the diameter of the axons and the presence or absence of the Remark bundle cannot be used to distinguish between afferent nerve fibers and efferent nerve fibers. The double-bilayer is a structural unit of the myelin sheath, and the myelin sheath formed by the MSCs is composed of multiple layers of double-bilayers. The myelin sheath (wrapped around the C-fiber in the Remark bundle) formed by NMSCs is composed of a single layer of double-bilayers. The compaction of the myelin sheath involves 2 steps. During the first step, the distance between the 2

layers of cell membranes in the double-bilayer becomes shorter, and during the second step, the adjacent double-bilayers are tightly closed to form the MDL. The expression level of MBP is positively correlated with the formation of the MDL. However, the anchoring of the myelin sheath by lipophilin particles might be required for the formation of a compacted myelin sheath. The abnormalities in nerve fiber structure observed in autologous nerve grafts do not appear to be related to either MBP or lipophilin, but to other factors, and further research is needed to explore these abnormalities and their causes.

Data Availability. All data discussed in the paper will be made available to readers.

ACKNOWLEDGMENTS. This study was supported by grants from the Chongqing Municipal Finance Special Fund Project (16403) and the China Scholarship Council (201806995007).

1. A. T. Campagnoni, C. W. Campagnoni, J. M. Bourre, C. Jacque, N. Baumann, Cell-free synthesis of myelin basic proteins in normal and dysmyelinating mutant mice. *J. Neurochem.* **42**, 733–739 (1984).
2. G. Shackleford *et al*., Involvement of Aryl hydrocarbon receptor in myelination and in human nerve sheath tumorigenesis. *Proc. Natl. Acad. Sci. U.S.A.* **115**, E1319–E1328 (2018).
3. C. B. Davenport, Hereditary tendency to form nerve tumors. *Proc. Natl. Acad. Sci. U.S.A.* **4**, 213–214 (1918).
4. E. McGlade-McCulloh, A. M. Morrissey, F. Norona, K. J. Muller, Individual microglia move rapidly and directly to nerve lesions in the leech central nervous system. *Proc. Natl. Acad. Sci. U.S.A.* **86**, 1093–1097 (1989).
5. P. J. Dyck, A. C. Lais, C. Giannini, J. K. Engelstad, Structural alterations of nerve during cuff compression. *Proc. Natl. Acad. Sci. U.S.A.* **87**, 9828–9832 (1990).
6. C. E. McMurran, C. A. Jones, D. C. Fitzgerald, R. J. Franklin, CNS remyelination and the innate immune system. *Front. Cell Dev. Biol.* **4**, 38 (2016).
7. S. K. Stumpf *et al*., Ketogenic diet ameliorates axonal defects and promotes myelination in Pelizaeus-Merzbacher disease. *Acta Neuropathol.* **138**, 147–161 (2019).
8. C. Matute, Characteristics of acute and chronic kainate excitotoxic damage to the optic nerve. *Proc. Natl. Acad. Sci. U.S.A.* **95**, 10229–10234 (1998).
9. S. S. Zamvil, L. Steinman, The T lymphocyte in experimental allergic encephalomyelitis. *Annu. Rev. Immunol.* **8**, 579–621 (1990).
10. I. Noorani, A. Lodge, G. Vajramani, O. Sparrow, The effectiveness of percutaneous balloon compression, thermocoagulation, and glycerol rhizolysis for trigeminal neuralgia in multiple sclerosis. *Neurosurgery* **85**, E684–E692 (2019).
11. S. Kim, J. C. Maynard, A. Strickland, A. L. Burlingame, J. Milbrandt, Schwann cell O-GlcNAcylation promotes peripheral nerve remyelination via attenuation of the AP-1 transcription factor JUN. *Proc. Natl. Acad. Sci. U.S.A.* **115**, 8019–8024 (2018).
12. R. D. Fields, Myelin formation and remodeling. *Cell* **156**, 15–17 (2014).
13. N. Snaidero *et al*., Myelin membrane wrapping of CNS axons by PI(3,4,5)P3-dependent polarized growth at the inner tongue. *Cell* **156**, 277–290 (2014).
14. K. M. Young *et al*., Oligodendrocyte dynamics in the healthy adult CNS: Evidence for myelin remodeling. *Neuron* **77**, 873–885 (2013).
15. J. M. Boggs, M. A. Moscarello, Structural organization of the human myelin membrane. *Biochim. Biophys. Acta* **515**, 1–21 (1978).
16. Y. Hu *et al*., Synergistic interactions of lipids and myelin basic protein. *Proc. Natl. Acad. Sci. U.S.A.* **101**, 13466–13471 (2004).
17. B. B. Geren, F. O. Schmitt, The structure of the Schwann cell and its relation to the axon in certain invertebrate nerve fibers. *Proc. Natl. Acad. Sci. U.S.A.* **40**, 863–870 (1954).
18. M. Brzin, The localization of acetylcholinesterase in axonal membranes of frog nerve fibers. *Proc. Natl. Acad. Sci. U.S.A.* **56**, 1560–1563 (1966).
19. P. R. Burton, J. L. Paige, Polarity of axoplasmic microtubules in the olfactory nerve of the frog. *Proc. Natl. Acad. Sci. U.S.A.* **78**, 3269–3273 (1981).
20. N. Okamura, M. Stoskopf, F. Hendricks, Y. Kishimoto, Phylogenetic dichotomy of nerve glycosphingolipids. *Proc. Natl. Acad. Sci. U.S.A.* **82**, 6779–6782 (1985).
21. L. L. Evans, P. C. Bridgman, Particles move along actin filament bundles in nerve growth cones. *Proc. Natl. Acad. Sci. U.S.A.* **92**, 10954–10958 (1995).
22. M. R. Wenk, P. De Camilli, Protein-lipid interactions and phosphoinositide metabolism in membrane traffic: Insights from vesicle recycling in nerve terminals. *Proc. Natl. Acad. Sci. U.S.A.* **101**, 8262–8269 (2004).
23. S. R. Detwiler, The effect of transplanting limbs upon the formation of nerve plexuses and the development of peripheral neurones. *Proc. Natl. Acad. Sci. U.S.A.* **5**, 324–331 (1919).
24. Y. Kidokoro, E. Yeh, Initial synaptic transmission at the growth cone in Xenopus nerve-muscle cultures. *Proc. Natl. Acad. Sci. U.S.A.* **79**, 6727–6731 (1982).
25. F. A. Rawlins, G. M. Villegas, E. T. Hedley-Whyte, B. G. Uzman, Fine structural localization of cholesterol-1,2- 3 H in degenerating and regenerating mouse sciatic nerve. *J. Cell Biol.* **52**, 615–625 (1972).
26. F. F. Ebner, R. S. Erzurumlu, S. M. Lee, Peripheral nerve damage facilitates functional innervation of brain grafts in adult sensory cortex. *Proc. Natl. Acad. Sci. U.S.A.* **86**, 730–734 (1989).
27. L. Maffei, G. Carmignoto, V. H. Perry, P. Candeo, G. Ferrari, Schwann cells promote the survival of rat retinal ganglion cells after optic nerve section. *Proc. Natl. Acad. Sci. U.S.A.* **87**, 1855–1859 (1990).
28. D. Kim *et al*., NADPH oxidase 2-derived reactive oxygen species in spinal cord microglia contribute to peripheral nerve injury-induced neuropathic pain. *Proc. Natl. Acad. Sci. U.S.A.* **107**, 14851–14856 (2010).
29. S. Tashiro, On the nature of the nerve impulse. *Proc. Natl. Acad. Sci. U.S.A.* **1**, 110–114 (1915).
30. J. H. Skene, E. M. Shooter, Denervated sheath cells secrete a new protein after nerve injury. *Proc. Natl. Acad. Sci. U.S.A.* **80**, 4169–4173 (1983).
31. J. D. Schmelzer, D. W. Zochodne, P. A. Low, Ischemic and reperfusion injury of rat peripheral nerve. *Proc. Natl. Acad. Sci. U.S.A.* **86**, 1639–1642 (1989).
32. C. Girard *et al*., Etifoxine improves peripheral nerve regeneration and functional recovery. *Proc. Natl. Acad. Sci. U.S.A.* **105**, 20505–20510 (2008).
33. G. Corfas, M. O. Velardez, C. P. Ko, N. Ratner, E. Peles, Mechanisms and roles of axon-Schwann cell interactions. *J. Neurosci.* **24**, 9250–9260 (2004).
34. S. Rotshenker, F. Reichert, E. M. Shooter, Lesion-induced synthesis and secretion of proteins by nonneuronal cells resident in frog peripheral nerve. *Proc. Natl. Acad. Sci. U.S.A.* **87**, 1144–1148 (1990).
35. M. L. Feltri, S. S. Scherer, L. Wrabetz, J. Kamholz, M. E. Shy, Mitogen-expanded Schwann cells retain the capacity to myelinate regenerating axons after transplantation into rat sciatic nerve. *Proc. Natl. Acad. Sci. U.S.A.* **89**, 8827–8831 (1992).
36. G. L. Barrett, P. F. Bartlett, The p75 nerve growth factor receptor mediates survival or death depending on the stage of sensory neuron development. *Proc. Natl. Acad. Sci. U.S.A.* **91**, 6501–6505 (1994).
37. B. H. Choi, R. C. Kim, Expression of glial fibrillary acidic protein in immature oligodendroglia. *Science* **223**, 407–409 (1984).
38. K. R. Jessen, R. Mirsky, Glial cells in the enteric nervous system contain glial fibrillary acidic protein. *Nature* **286**, 736–737 (1980).
39. C. Readhead *et al*., Expression of a myelin basic protein gene in transgenic shiverer mice: Correction of the dysmyelinating phenotype. *Cell* **48**, 703–712 (1987).
40. A. Privat, C. Jacque, J. M. Bourre, P. Dupouey, N. Baumann, Absence of the major dense line in myelin of the mutant mouse "shiverer". *Neurosci. Lett.* **12**, 107–112 (1979).
41. T. D. Bird, D. F. Farrell, S. M. Sumi, Brain lipid composition of the shiverer mouse: (genetic defect in myelin development). *J. Neurochem.* **31**, 387–391 (1978).
42. J. Rosenbluth, Peripheral myelin in the mouse mutant Shiverer. *J. Comp. Neurol.* **193**, 729–739 (1980).
43. F. de Ferra *et al*., Alternative splicing accounts for the four forms of myelin basic protein. *Cell* **43**, 721–727 (1985).
44. A. Roach, N. Takahashi, D. Pravtcheva, F. Ruddle, L. Hood, Chromosomal mapping of mouse myelin basic protein gene and structure and transcription of the partially deleted gene in shiverer mutant mice. *Cell* **42**, 149–155 (1985).
45. A. O. Valdivia, V. Farr, S. K. Bhattacharya, A novel myelin basic protein transcript variant in the murine central nervous system. *Mol. Biol. Rep.* **46**, 2547–2553 (2019).
46. A. Roach, K. Boylan, S. Horvath, S. B. Prusiner, L. E. Hood, Characterization of cloned cDNA representing rat myelin basic protein: Absence of expression in brain of shiverer mutant mice. *Cell* **34**, 799–806 (1983).
47. N. Takahashi, A. Roach, D. B. Teplow, S. B. Prusiner, L. Hood, Cloning and characterization of the myelin basic protein gene from mouse: One gene can encode both 14 kd and 18.5 kd MBPs by alternate use of exons. *Cell* **42**, 139–148 (1985).
48. R. E. Martenson, G. E. Deibler, M. W. Kies, The occurrence of two myelin basic proteins in the central nervous system of rodents in the suborders Myomorpha and Sciuromorpha. *J. Neurochem.* **18**, 2427–2433 (1971).
49. D. R. Beniac *et al*., Three-dimensional structure of myelin basic protein. I. Reconstruction via angular reconstitution of randomly oriented single particles. *J. Biol. Chem.* **272**, 4261–4268 (1997).
50. E. Polverini, E. P. Coll, D. P. Tieleman, G. Harauz, Conformational choreography of a molecular switch region in myelin basic protein—Molecular dynamics shows induced folding and secondary structure type conversion upon threonyl phosphorylation in both aqueous and membrane-associated environments. *Biochim. Biophys. Acta* **1808**, 674–683 (2011).
51. L. Yang, D. Tan, H. Piao, Myelin basic protein citrullination in multiple sclerosis: A potential therapeutic target for the pathology. *Neurochem. Res.* **41**, 1845–1856 (2016).
52. H. Hydén, A calcium-dependent mechanism for synapse and nerve cell membrane modulation. *Proc. Natl. Acad. Sci. U.S.A.* **71**, 2965–2968 (1974).
53. E. Schoffeniels, G. Dandrifosse, Protein phosphorylation and sodium conductance in nerve membrane. *Proc. Natl. Acad. Sci. U.S.A.* **77**, 812–816 (1980).
54. M. A. Ahmed *et al*., Solution nuclear magnetic resonance structure and molecular dynamics simulations of a murine 18.5 kDa myelin basic protein segment (S72-S107) in association with dodecylphosphocholine micelles. *Biochemistry* **51**, 7475–7487 (2012).
55. P. P. da Silva, R. G. Miller, Membrane particles on fracture faces of frozen myelin. *Proc. Natl. Acad. Sci. U.S.A.* **72**, 4046–4050 (1975).
56. A. Gow, Redefining the lipophilin family of proteolipid proteins. *J. Neurosci. Res.* **50**, 659–664 (1997).